

Correlations and fluctuations in multiparticle production

I. M. Dremin

P. N. Lebedev Physics Institute, Academy of Sciences of the USSR
Sov. Phys. Usp. **160**, 105–133 (August 1990)

A review of the experimental data on correlations and number fluctuations in multiparticle production at high energies. The author discusses new concepts of intermittency and fractality that can be used to describe these processes.

1. INTRODUCTION

When two particles collide at very high energies the most probable outcome is the production of a large number of new particles. Studies of multiparticle production processes began more than 50 years ago with cosmic ray research and many scientists are active in this field today. The most complete and precise results have been obtained in experiments at particle accelerators, which continue to extend the overlap of the energy range previously accessible only in cosmic ray studies. Despite the enormous accumulations of experimental data and our increasing experience in constructing phenomenological models, we still cannot explain all observed phenomena or predict new properties. The advances achieved in the past quarter century in deciphering the quark structure of strong interactions have yet to resolve the fundamental questions of multiparticle production, although we now possess new phenomenological models that correctly reproduce many properties of inelastic processes. Nonetheless, we are often faced with experimental surprises that compel us to modify or even abandon our theoretical models. In the review we will discuss one such surprise.

Investigations of multiparticle production processes usually proceed from the simplest characteristics: total cross-sections, multiplicity distributions, single-particle inclusive (pseudo) rapidity and transverse momenta, distributions, etc. More detailed information can be obtained from correlation measurements and exclusive experiments that require great effort and improved experimental apparatus. The accumulation of the resulting information helps to clarify the dynamics of the processes in question.

From the viewpoint of a theorist, experimental results are best approached via quantum chromodynamics (QCD). Unfortunately, the application of QCD to soft processes involving small momentum transfers is quite restricted. The problem lies in our insufficient understanding of the quark nonemission mechanism that is produced by strong nonperturbative effects. In the theory of multiparticle production this problem requires us to resort to phenomenological descriptions of the transformation of QCD quarks and gluons into the experimentally observed hadrons. Hence we are compelled either to construct general relations that connect various experimental facts or to develop phenomenological models that describe these facts by adjusting a number of free parameters. By now many such models have been developed. These usually employ Monte Carlo simulations to extract complete information on all produced particles. Occasionally a model proves incapable of explaining new experimental results or becomes invalid in a newly accessible energy range. Such a model is either modified or altogether abandoned.

The fluctuation problem was the downfall of all earlier models, since none of them could explain the experimental results.

The dynamics of these fluctuations is the subject of much current debate. Various hypotheses have been proposed, all invoking either chaotic (intermittent) dynamics or the usual (but of a special type) dynamical processes.

In this review we shall briefly describe the general picture of particle correlations in hadron production processes and concentrate on experimental results on fluctuations, their connection with observed correlations, and the theoretical approaches to fluctuation dynamics. The purpose of the review is to present the fundamental principles and ideas in a concise form, allowing the reader the freedom to delve further into the numerous studies in this field that have appeared recently and are cited in the references. The burgeoning interest in this subject has led to ever-increasing amount of experimental and theoretical research, accompanied by the appearance of many new and interesting problems.

2. CORRELATIONS

Like all many-body problems, multiparticle production possesses an enormous number of characteristics that contain information on particle correlations. Indeed, any process that produces n particles can be described by a collection of n points in three-dimensional phase space, with each point labeling the properties of the appropriate particle (mass, charge, spin, etc.). Correspondingly, the number and variety of the correlations is enormous; two-, three- or many-particle correlations; azimuthal correlations; distributions over rapidity bins containing several particles; correlations of particle groups in various phase space domains; etc. In this review we shall restrict ourselves, for the most part, to (pseudo) rapidity correlations of produced particles, neglecting charge correlations, correlations of different types of particles, etc.

Clearly, the existence of correlations is evident in the simplest properties of particle production processes, for example the multiplicity distribution in the various domains of the accessible phase space and the behavior of the higher moments of this distribution. The well-known phenomenological description of the distributions of inelastic processes over the multiplicity n in the total phase space employs the scale-invariant KNO (Koba–Nielsen–Olesen) distribution

$$P(n) = \frac{1}{\langle n \rangle} \psi \left(\frac{n}{\langle n \rangle} \right) \quad (1)$$

(ψ is a universal function that does not depend explicitly on energy). This description has been quite successful for electron-positron annihilation, lepton production at all currently accessible energies (up to $s^{1/2} \sim 50$ GeV), as well as ha-

dron-hadron processes up to the highest ISR energies ($s^{1/2} \sim 63$ GeV). However, at even higher energies attainable at the Sp \bar{p} S and FNAL colliders (up to $s^{1/2} \sim 900$ GeV and 1.8 TeV, respectively) the scale invariance ensured by ψ being only a function of the ratio of multiplicity n to the average multiplicity $\langle n \rangle$ breaks down, and the distributions broaden with increasing energy. The peak at small multiplicities becomes sharper and higher, but the role of processes with significantly above-average multiplicities also increases. This is illustrated in Fig. 1, which compares the experimental results on nondiffractive $p\bar{p}$ -processes at 200 and 900 GeV in terms of KNO units of $n/\langle n \rangle$ (the logarithmic and linear scales of the ordinate axes emphasize different properties of these distributions).

The correlation-induced breakdown of KNO scaling clearly manifests itself in the behavior of the normalized moments of the multiplicity distribution

$$C_q = \frac{\langle n^q \rangle}{\langle n \rangle^q}, \quad (2)$$

which should be independent of energy as long as KNO scaling remains valid. Experimentally these moments indeed remain nearly constant up to ISR energies, but they increase markedly in colliders over the total rapidity window (Fig. 2) while falling off in small rapidity bins in the central region.

To remedy this discrepancy several other parametrizations with more fitting parameters have been proposed, the most popular being the negative binomial distribution. Yet even the latter failed to describe the measured multiplicity distribution of charged particles in $p\bar{p}$ -interactions at $s^{1/2} = 900$ GeV.

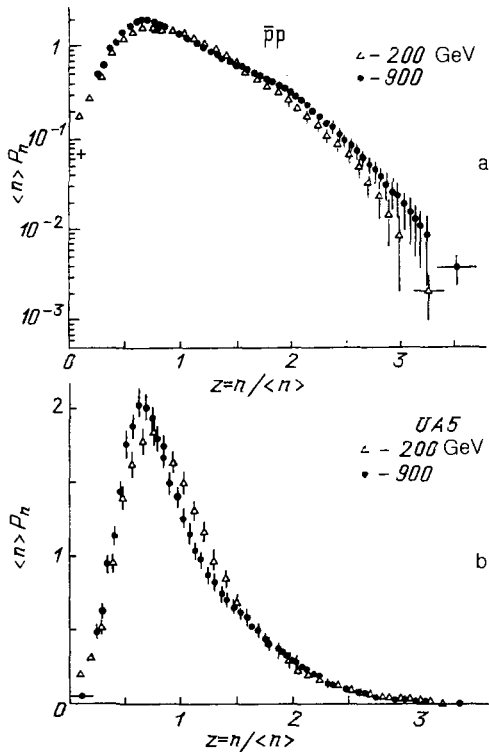


FIG. 1. Multiplicity distributions in nondiffractive $p\bar{p}$ -interactions at 200 GeV and 900 GeV center-of-mass energies that demonstrate deviations from KNO scaling at these energies. The scales are logarithmic (a) and linear (b).

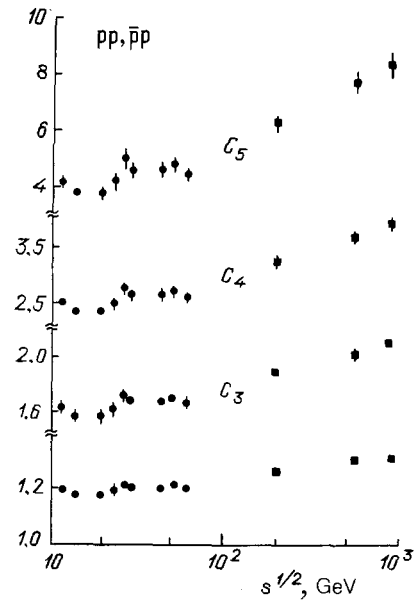


FIG. 2. Normalized moments of multiplicity distributions as a function of initial energy (the lowest set of points is C_2).

Before discussing (pseudo) rapidity correlations, let us briefly mention several other, widely discussed correlations. Charge correlations may be manifested in large number-fluctuations of charged and neutral pions produced in a given event if the ratio of charged to neutral pions departs significantly from two, which is the expected value in the absence of correlations. Experimental evidence includes the observation of anomalous events in cosmic rays with few neutral particles (Centaur and mini-Centaur) and, conversely, in rays containing unusually large numbers of γ -quanta (gammanization). Long-range correlations enter into the linear dependence of the average multiplicity of particles emitted into the backward hemisphere on the number of particles emitted into the forward hemisphere. There is also the correlation of the mean transverse and the longitudinal momentum of the produced particles, known as the "seagull effect". The problem of quark-gluon plasma formation has stimulated research into correlations between the mean transverse momentum and the particle number density on the rapidity axis. More pertinent to the subject of this review is the Bose-Einstein correlation, which establishes an attraction between two identical bosons (pions) in rapidity space.

Moving on to our subject of (pseudo) rapidity correlations, let us begin by defining the kinematic variables and the form of single-particle inclusive spectra. The simplest method of treating an inelastic event as a one-dimensional problem consists of projecting all particles (points in the phase space) onto the rapidity axis:

$$y = \frac{1}{2} \ln \frac{\varepsilon + p_l}{\varepsilon - p_l}, \quad (3)$$

(where ε and $p_l = p \cos \theta$ are the particle energy and longitudinal momentum in the center-of-mass coordinates). Alternatively, the particles can be projected onto the (pseudo) rapidity axis:

$$\eta = - \ln \operatorname{tg} \frac{\theta}{2}, \quad (4)$$

which coincides with ordinary rapidity for relativistic parti-

cles emitted at small angles θ .

Hereafter we will focus mainly on hadron-hadron processes, although electron-positron annihilation and nucleus-nucleus interactions will receive occasional mention.

Inclusive (pseudo) rapidity distribution of particles usually appears either bell-shaped or hat-like with a dimple at the center. In the first approximation it is taken to be a plateau whose height and width increase with energy. The increase in height is more rapid than the attendant increase in the total cross-section, while the width of the distribution increases more slowly than the broadening of the total rapidity window permitted by the conservation laws. Phenomenological fits of the energy dependence of the distribution height (divided by the total cross-section) are as follows:

$$\begin{aligned} \rho(0) &= \frac{1}{\sigma} \frac{d\sigma}{d\eta} \Big|_{\eta=0} \\ &= 0.01 + 0.22 \ln s \quad \text{logarithmic approximation} \\ &= 0.744 s^{0.105} \quad \text{power-law approximation} \end{aligned} \quad (5)$$

Rapidity correlations of two secondary particles contain a strong short-range term. The correlation function

$$R(y_1, y_2) = \frac{\frac{1}{\sigma} \frac{\partial^2 \sigma}{\partial y_1 \partial y_2}}{\frac{1}{\sigma} \frac{\partial \sigma}{\partial y_1} \frac{1}{\sigma} \frac{\partial \sigma}{\partial y_2}} - 1 \quad (6)$$

has a maximum when the particle rapidities are equal, $y_1 = y_2$; the width of this maximum $\Delta y \approx 2$. This is illustrated in Fig. 3, where we plot the rapidity correlations of two charged (cc), negative (— —), positive (++), and positive plus negative (— +) particles. The experimental data (points) are complemented by theoretical curves obtained from Monte Carlo ensembles of events according to the dual parton model¹ of the Orsay group (MCDPM),¹ the generalized cluster model of the UA5 collaboration (GENCL),² and the Fritiof model of the Lund group (FRITIOF).³ Es-

entially, the GENCL cluster model is purely phenomenological, since the inputs consist of experimental data on multiplicity and rapidity distributions. It is not surprising, therefore, that it is the most successful in reproducing two-particle correlations, which are partially present in the inputs, by introducing a clustering mechanism that requires additional two-particle attraction (although there are some problems in the case of two negatively charged particles—see Fig. 3). The other models are based on theoretical descriptions of the processes and yield weaker correlations than are actually observed, although the results are qualitatively similar to experimental data.

We note here that analogous problems arose earlier in investigations of the simplest multiperipheral models.⁴ These problems could only be resolved by “manually” introducing strong correlations within certain groups of particles labeled as clusters (or, earlier still, fireballs), that had greater masses than the known resonances. The recent efforts to promote the application of quantum chromodynamics from hard to semi-soft and soft processes have led to the introduction of minijets that are conceptually similar to clusters (fireballs).

At the same time, direct experimental information on many-particle correlations is still very meager. The investigation of three-particle correlation functions by generalizing (6) is hindered both by the large number of variables and by their less explicit effect on the final result. We do know, however, that three-particle correlations increase with energy⁴ between 50 and 400 GeV. Later we will see how more explicit information on actual many-particle correlations can be extracted from fluctuations.

3. FLUCTUATIONS

Multiparticle production processes do not uniformly fill the phase space allowed by conservation laws with secondary particles. Large transverse momenta are strongly suppressed, while the longitudinal momentum distribution is determined by the inclusive rapidity distribution. Because of this a cylindrical phase volume is often assumed. Yet in

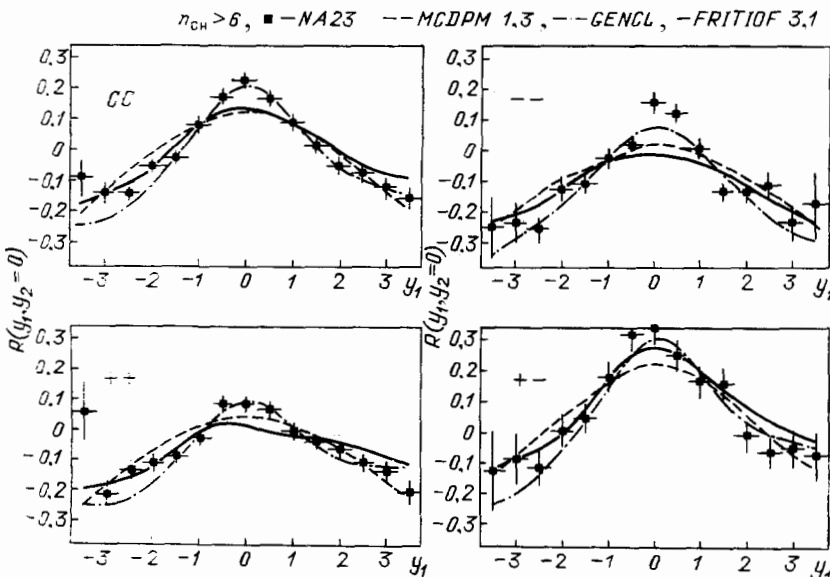


FIG. 3. Two-particle correlations of arbitrarily charged particles (cc), negatively charged particles (— —), positively charged particles (++), and oppositely charged particles (— +).

single events the particles are not as uniformly distributed even in this cylindrical phase volume as required by the inclusive distribution. This would not be altogether surprising if the deviations from inclusive distribution curves were due to the finite statistics of a given event. On the other hand, if these deviations (fluctuations) cannot be explained by statistical effects alone, their existence indicates the presence of some dynamical mechanisms that determine fluctuation properties. A general approach to the fluctuation problem seeks to uncover the dynamics of the processes by studying fluctuation properties.

Relatively long ago, physicists investigating cosmic rays reported inelastic events with unexpectedly large particle number fluctuations confined to very narrow pseudorapidity bins. Subsequently such events were observed and carefully studied at particle accelerators.^{8,9} One event is reproduced in Fig. 4. A very narrow rapidity bin $\Delta y = 0.1$ contains ten charged particles, a factor of approximately 40 larger than the mean inclusive density $\rho(y)$.

As the total rapidity window is reduced, the multiplicity distribution normalized by the bin-averaged number of particles per bin (i.e. expressed in KNO variables) becomes wider as the bin size decreases. This indicates fluctuation enhancement. The first obvious question is whether this effect can be understood in the simplest cases, where fluctuations are either purely statistical or driven by weak pair correlations, like fluctuations in dilute gases. In this regard, consider a fluctuation in the rapidity distribution of particles $\rho_e(y)$ produced in a given event. We define a fluctuation with respect to the inclusive distribution as follows:

$$\varepsilon(y) = \frac{\rho_e(y)}{\rho(y)} - 1. \quad (7)$$

In systems with weak pair correlations the behavior of this fluctuation obeys the Gaussian law

$$P[\varepsilon(y)] = \frac{1}{N} \exp \left[-\frac{1}{2} \int dz_1 dz_2 \varepsilon(z_1) R^{-1}(|z_1 - z_2|) \varepsilon(z_2) \right], \quad (8)$$

where²⁾

$$N = \int [d\varepsilon(y)] \exp \left[-\frac{1}{2} \int dz_1 dz_2 \varepsilon(z_1) R^{-1}(|z_1 - z_2|) \varepsilon(z_2) \right] \quad (9)$$

with $R(z_1 - z_2)$ given by formula (6).

Experimentally, in a given event there is some probability of observing k peaks exceeding some threshold t located at points y_i ($i = 1, \dots, k$). In order to calculate this probability one computes the functional integral

$$P_k(y_i) = \int_t^\infty dr_1 \dots \int_t^\infty dr_k \int [d\varepsilon] P[\varepsilon] \prod_{i=1}^k \delta(\varepsilon(y_i) - r_i). \quad (10)$$

If the threshold t is set sufficiently high (very dense groups of particles), a single event will contain either one such peak or none at all. Consequently, we can obtain the probability of strong fluctuations from a single term

$$P_1 = \left(\frac{R(0)}{2\pi} \right)^{1/2} \frac{\exp(-t^2/2R(0))}{t} \sum_{m=0}^{\infty} (-1)^m (2m-1)!! \left(\frac{R(0)}{t^2} \right). \quad (11)$$

Evidently, the Gaussian distribution reappears in a slightly modified form but with a definite exponent. A comparison of this distribution with the experimental results obtained by the NA22 collaboration is shown in Fig. 5. Experimentally the number of fluctuations falls exponentially with peak height, whereas the theory predicts a much sharper decay. Hence it follows that we are either dealing with real many-particle correlations that cannot be reduced to pair correlations, or that the pair correlations are so strong that they produce sizable many-particle correlations by multiple pairing (see Refs. 4). The latter hypothesis was developed in Refs. 11, 12—we shall return to it below. For now let us point out that Monte Carlo modeling of fluctuations in the dual parton¹³ and Fritiof¹⁴ models demonstrated that our theoretical picture again cannot explain the experimental results, since the number of fluctuations predicted by these models is considerably smaller and their decay with increasing peak height is considerably faster than what is actually observed (see Fig. 5). It is likely that fluctuations were the first striking experimental fact that could neither be explained by theoretical models nor accounted for by adjusting the model parameters, although as we have already discussed the (less dramatic) two-particle correlation problem had not been theoretically resolved either.

Clearly, fluctuations are a manifestation of many-particle correlations and the central problem is to describe their dynamical evolution. To this end several approaches have been proposed. In addition to the traditional suggestions of reducing this problem to known results (for example, expressing all correlations in terms of two-particle correla-

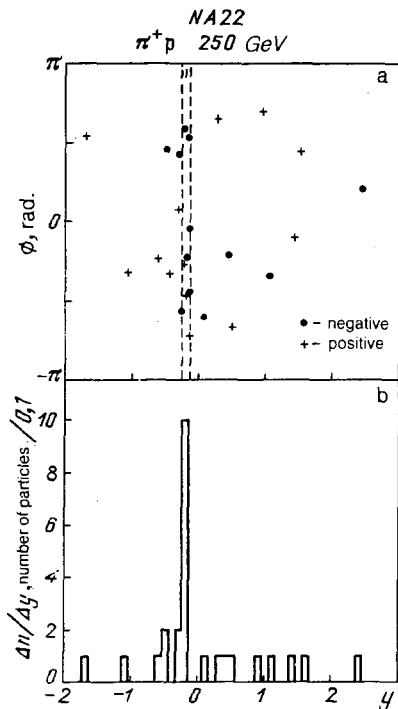


FIG. 4. A π^+ p-interaction event at 250 GeV that produced 10 particles in a narrow rapidity range $\Delta y = 0.1$ (a) and the corresponding histogram of particle rapidity distribution (b).⁹

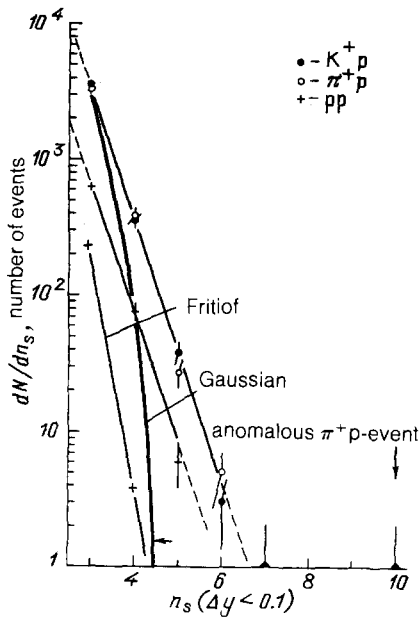


FIG. 5. Experimental multiplicity distribution in groups containing a fixed number of particles n in a bin $\Delta y = 0.1$ for π^+ p-interactions at 250 GeV (points).⁹ The solid curve is the Gaussian parametrization (11);¹⁰ the dashed curve is the result of the FRITIOF model.¹⁴

tions) or uncovering some heretofore neglected properties of existing theoretical models, there have been hypotheses about stochastic dynamics of multiparticle production related to intermittency and fractality, similar to turbulence. Since the latter concepts have only recently been introduced to particle physics, we shall briefly define both in the following sections. We will find that the two ideas are closely linked, although I believe fractality is somewhat more far-reaching, since it follows directly from the geometrical properties of an object or from distributions over it.

4. INTERMITTENCY AND FACTORIAL MOMENTS

The concept of intermittency has been borrowed from the theory of turbulence. There it represents the following important property of a turbulent liquid: vortices of different size alternate in such a manner as to form a self-similar structure. Mathematically this property is defined by a power-law dependence of the vortex distribution moments on the vortex size.

When intermittency is applied to multiparticle production,¹⁵ it is defined analogously to turbulence theory as the power-law increase of multiplicity distribution moments over rapidity bins as the bin size is reduced. Clearly in order to extract the dynamical behavior one must exclude the purely statistical fluctuations due to the finite number of particles in the problem. This is particularly important in studying small bins, where the number of particles can be very low. A method of suppressing statistical fluctuations was proposed in Ref. 15. We are interested solely in the behavior of real distribution moments averaged over dynamic fluctuations only. Experimentally, however, we cannot distinguish real dynamical fluctuations from statistical ones, and the measured characteristics are therefore averaged over both types of fluctuations. Bialas and Peschanski dem-

onstrated¹⁵ that if the statistical fluctuations can be described by the Bernoulli distribution, then the factorial moments calculated from experimental data are identical to real moments averaged over dynamical fluctuations only. In this case, the factorial moment or order q of the multiplicity distribution over rapidity bins of size δy can then be written as follows:³⁾

$$F_q(\delta y) = M^{q-1} \frac{\left\langle \sum_{k=1}^M n_k (n_k - 1) \dots (n_k - q + 1) \right\rangle}{\langle n \rangle^q}, \quad (12)$$

where M is the number of bins of width δy in the total rapidity window Y (i.e. $Y = M\delta y$); averaging is carried out over all events; n_k is the number of particles in bin k .

Assuming the factorial moments defined in (12) are identically equal to real moments averaged over dynamical fluctuations, we can define intermittency (analogously to the procedure for a turbulent liquid) as the power-law dependence of factorial moments on bin size:

$$F_q(\delta y) \sim (\delta y)^{-\varphi(q)}, \quad (13)$$

that is, $\ln F_q$ increases linearly with $-\ln \delta y$ for a given q . Note that the ordinary moments C_q [see formula (2)] must approach a constant¹⁷ if the average multiplicity in a narrow bin is smaller than unity. The formulae (12) and (13) are valid if the interval falls within the plateau. Outside the plateau, F_q should be divided by

$$R_q(\delta y) = \frac{1}{M} \sum_{k=1}^M \rho_k^q \left(\frac{1}{M} \sum_{k=1}^M \rho_k \right)^{-q}.$$

Factorial moments have been calculated from experimental results of many reactions at various energies. The values of parameters $\varphi(q)$, known as slope parameters, turn out to be relatively small (several-fold smaller than values characteristic of full-blown turbulence), but clearly different from zero, at least in the $0.1 < \delta y < 1$ region. The linear increase of F_q with δy is shown on logarithmic axes in Fig. 6, with experimental data taken from the NA22 collaboration that studied π^+ p-interactions at 250 GeV. Physically the enhancement of factorial moments in smaller rapidity bins is a consequence of fluctuations characterized by large particle densities. The general tendencies in the behavior of the slope parameters can be summarized as follows (see a review by Kittel and Peschanski,¹⁸ who compiled an exhaustive reference list of experimental and theoretical studies⁴⁾):

- 1) $\varphi(q)$ increase with q ;
- 2) for the same initial energy the intermittency powers $\varphi(q)$ are greater in electron-positron annihilation than in hadron interactions; in turn, the latter are greater in nucleus-nucleus interactions;
- 3) $\varphi(q)$ decrease with energy;
- 4) at a given energy $\varphi(q)$ decrease as the multiplicity increases;
- 5) $\varphi(q)$ decrease as the transverse momentum increases;
- 6) $\varphi(q)$ are smaller if the analysis is one-dimensional (rapidity bins only) rather than two-dimensional (rapidity bins and azimuthal angle windows);
- 7) experimental values of $\varphi(q)$ are larger than predicted by Monte Carlo simulations based on MCDPM and FRITIOF models;

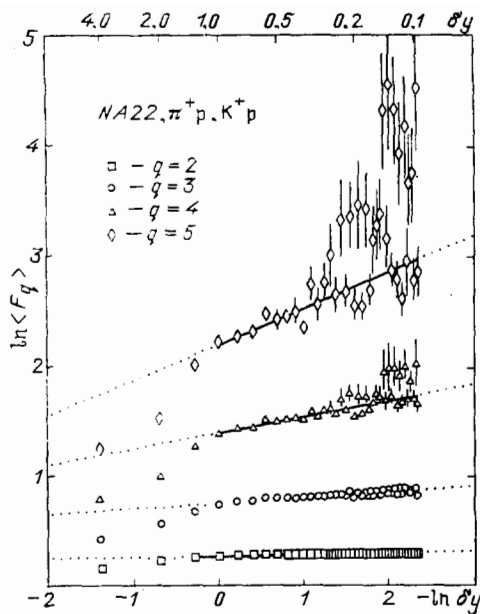


FIG. 6. Factorial moments as functions of the rapidity bin size in $\pi^+ p$ -interactions at 250 GeV.

8) values of $\varphi(q)$ are practically independent of the charge of secondary particles.

Although the notion of calculating factorial moments arose by analogy with turbulence because of indications that chaotic dynamics play an important role, first it is of interest to consider what our standard picture would predict for the behavior of these moments and how these predictions compare with experimental results. We have already seen (property 7) that slope parameters predicted by the standard theories^{1,3} underestimate the importance of fluctuations in experimental data. This is possibly due to an insufficient description of two-particle correlations or an inadequate treatment of Bose-Einstein correlations. However, the weak dependence of the intermittency powers on particle charge (property 8) seems to indicate that the role of Bose-Einstein correlations is relatively weak, although they have been occasionally invoked to interpret experimental intermittency results.¹⁹ Note that theoretical predictions of Ref. 19 require the slope parameters for particles of the same charge to be twice as large as for oppositely charged particles.

In this connection we should note Ref. 20, which demonstrated the Bose-Einstein correlations can be significantly enhanced above the limiting values usually employed in calculations. Moreover, the links between channels for producing oppositely charged particles and their consequently wide distribution²¹ could markedly alter the ratio of their slope parameters. This question requires further study.

As we have discussed earlier, two-particle correlations evidently do not suffice to explain the observed fluctuations, which require a contribution from many-particle correlations. Significant progress in understanding the dynamics of multiparticle production could be made if the experimental results could be explained by expressing many-particle correlations in terms of two-particle correlations. Naturally, this was attempted by various authors.^{11,12} In these studies many-particle correlations were expressed as products of two-particle correlations which, in turn, were approximated

by simple or Gaussian exponential terms. The authors of Refs. 11, 12 claimed that the proper selection of fitting parameters brings these approximations into good agreement with the observed behavior of factorial moments. Yet an examination of the approximations involved casts doubt on the reliability of the fitting parameters and the feasibility of quantitative descriptions at various energies. The exponential parametrization of two-particle correlations employed by both groups^{11,12} is known to give a sharp peak in narrow rapidity bins at high energies $s^{1/2} \gtrsim 200$ GeV (the conclusions of Refs. 11 and 12 differ somewhat on this point), which is not in good agreement with experiment. Capella and coworkers¹² had problems in describing the lowest factorial moment $F_2(\delta y)$, whereas Carruthers and Sarcevic¹¹ succeeded in describing the experimental results completely (except for higher moment irregularities in small bins). The Gaussian parametrization of Ref. 12 proved less accurate in describing factorial moments, although it is more suitable for two-particle correlations. A careful examination of the plots in Ref. 12 shows that in small bins the calculated slope parameters are practically zero, and hence considerably smaller than experimental values. This agrees with the earlier result¹⁵ that factorial moments become bin-independent for Gaussian clusters that are broader than the bin size. Consequently, while the conclusion that many-particle correlations play an important role in fluctuations is beyond doubt, the actual form of these many-particle correlations remains to be established. Also, the decomposition of many-particle correlations into two-particle correlations sheds no light on the dynamics of the former. In particular, it is quite possible that it is precisely the many-particle correlations which lead to intermittency in cascade models.

The slope parameters are the simplest parameters of many-particle correlations. In principle, they can be replaced by other, possibly more convenient quantities.

Essentially, factorial moments are determined by multiplicity distributions $p_n(\delta y)$ over given bin sizes δy :

$$F_q(\delta y) \sim \left\langle \frac{\sum_n n(n-1)\dots(n-q+1)P_n(\delta y)}{\left(\sum_n P_n(\delta y)\right)^q} \right\rangle. \quad (14)$$

They can be calculated easily for the negative binomial distribution, for example. This distribution is characterized by two parameters, $\langle n \rangle$ and k , and has the form

$$P(n, \langle n \rangle, k) = \frac{\Gamma(n+k)}{\Gamma(n+1)\Gamma(k)} \frac{(\langle n \rangle/k)^n}{[1 + (\langle n \rangle/k)]^{n+k}}, \quad (15)$$

The resulting factorial moments depend only on $k(\delta y)$:

$$\begin{aligned} F_2 &= 1 + k^{-1}, \\ F_3 &= (1 + k^{-1})(1 + 2k^{-2}), \\ F_4 &= (1 + k^{-1})(1 + 2k^{-2})(1 + 3k^{-3}) \dots \end{aligned} \quad (16)$$

Consequently, the dependence of k on δy determines the behavior of all factorial moments. This assumption about multiplicity distributions yields good agreement with experimental results. Hence it turns out that all measured moments can be reproduced from a single moment. The parametrization indicates that the properties of many-particle

correlations are determined by a single function $k(\delta y)$. Note that this parametrization is only approximate because the product of two generating functions of the negative binomial distribution over two adjacent bins does not yield a correct generating function for the sum of these two bins. Still, as long as only the distribution tails are important, the negative binomial distribution is well-approximated by the gamma-distribution, which does yield the correct function for a summed bin, thus avoiding the contradiction.

To conclude, factorial moments characterize the multiplicity distribution by averaging over certain domains in the phase space and depend on the extent of these domains. Obviously any model that accurately describes multiplicity distributions will also predict the behavior of factorial moments. The advantage of studying factorial moments instead of the usual multiplicity distributions lies in their emphasis on the improbable but strong dynamical fluctuations and the useful analogies with turbulence.

5. FRACTALITY

A more profound and unified description of experimental results can be reached by invoking the concept of fractals. The power-law behavior of distribution moments as a function of bin size indicates that either the object itself or the distributions over the object have some fractal structure. Furthermore, the properties of the distribution moment parameters are linked with the dynamics of the appearance of self-similarity, which permits phase transitions at certain values of these parameters.

Fractals are self-similar objects of nonintegral dimension. The fractal dimension is a generalization of ordinary topological dimensionality to nonintegers. At first, it appears difficult to visualize a fractal object if dimensionality is taken to mean the number of independent measurements (or directions) which characterize a given object. Yet if one reverts to the definitions of Kolmogorov or Hausdorff the situation becomes transparent. They define the fractal dimension D_F to be the quantity which gives a finite limit

$$0 < \lim_{\varepsilon \rightarrow 0} N(\varepsilon) \varepsilon^{D_F} < \infty \quad (17)$$

for the product of the minimal number of hypercubes $N(\varepsilon)$ of linear extent $l = \varepsilon$ (Kolmogorov definition) or $l \leq \varepsilon$ (Hausdorff definition)⁵⁾ required to cover the object and the quantity ε^{D_F} as $\varepsilon \rightarrow 0$.

This definition becomes more physically intuitive if the mass (M) of the object is taken to depend on the linear extent l by the power-law

$$M \sim l^{D_F}. \quad (18)$$

We are accustomed to objects for which D_F coincides with topological dimensionality (for a line $D_F = 1$; for a square $D_F = 2$; for a cube $D_F = 3$; etc.). Yet objects with nonintegral D_F are not so rare in everyday existence. Our lungs, the clouds, the coastline, polymers, and, generally, any object with complex self-similar structure—all of these are fractals.

Consider some geometrical figures that have fractal structures. First, construct a Koch curve according to the following algorithm. A line segment is divided into three equal parts, an equilateral triangle is built using the middle part, and then the base of the triangle is erased. This procedure is repeated with each of the remaining four segments,

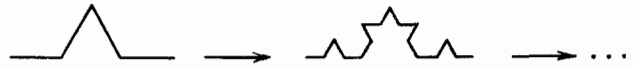


FIG. 7. The Koch curve is obtained by an iterative procedure, the first steps of which are shown in this figure.

etc. The resulting self-similar curve (Fig. 7) has a fractal dimension $D_F = \ln 4 / \ln 3 \approx 1.26$, as can be easily verified from expression (18).

If in the preceding example we simply drop the middle segment and repeat the tripartite division we arrive at the so-called Cantor set (Fig. 8) of an infinite number of points with dimension $D_F = \ln 2 / \ln 3 \approx 0.63$.

Analogous procedures exist for two- and three-dimensional objects. The resulting fractals can have dimensionalities that are both larger and smaller than those of the original objects.

At small l , the probability $p_i(l)$ of belonging to a given (i th) hypercube out of their total number $N(l)$ is proportional to l^{D_F} . As a result, the sum of the moments in a fractal is

$$\sum_i p_i^q(l) \sim l^{q D_F} \quad (D_F = \text{const}). \quad (19)$$

One can envisage more complicated self-similar objects consisting of differently weighted fractals with different dimensionalities. Such objects are called multifractals and for them

$$\sum_i p_i^q(l) \sim l^{\phi(q)}, \quad (20)$$

where

$$\phi(q) = q d_{q+1}. \quad (21)$$

The quantity d_{q+1} is known as the Renyi dimension²³ (or generalized dimension). It depends on q ; in fact, it can be shown²² that it must be a decreasing function of q .

Sometimes it is more convenient to characterize multifractals not by dimensionality, but rather by spectral properties. The spectral function $f(\alpha)$ is defined by the number of hypercubes required to cover the subset $S(\alpha)$ with the same probability behavior $p_i \sim l^\alpha$ ($l \rightarrow 0$):

$$dN_\alpha(l) = d\rho(\alpha) l^{-f(\alpha)}. \quad (22)$$

The Renyi dimension is related to the spectral function by the following expression

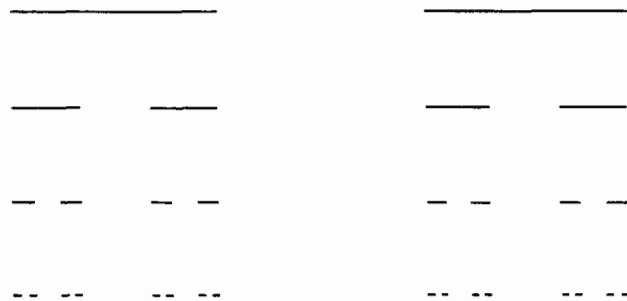


FIG. 8. The Cantor set is obtained by an iterative procedure, the first steps of which are shown in this figure.

$$\sum_i^{N(l)} p_i^q(l) \sim \int d\rho(\alpha) l^{\alpha q - f(\alpha)}, \quad (23)$$

which leads, by the steepest descent method, to

$$d_q = \frac{1}{q-1} \min_{\alpha} (\alpha q, f(\alpha)) = \frac{1}{q-1} (\bar{\alpha} q - f(\bar{\alpha})) \quad (24)$$

with α defined by

$$\left. \frac{df}{d\alpha} \right|_{\bar{\alpha}} = q(\bar{\alpha}) \quad (25)$$

as long as

$$\left. \frac{d^2f}{d\alpha^2} \right|_{\bar{\alpha}} < 0. \quad (26)$$

The spectral function $f(\alpha)$ is widely used in the analysis of multifractals. Neglecting the finer details (see Ref. 22 for a more detailed description), let us note one of its fundamental properties: if the spectral function is linear over some interval, this could indicate a phase transition that is difficult to detect by other means. It is also worth noting that there exists a well-developed thermodynamic formalism for multifractals that emphasizes their close analogy to spin systems.²² The Renyi dimension generalizes several concepts proposed for different applications, such as the fractal dimension

$$d_0 = D_F = -\phi(-1), \quad (27)$$

information dimension

$$d_1 = D_1 = \phi'(0), \quad (28)$$

and correlation dimension

$$d_2 = \nu = \phi(1) \quad (29)$$

with the general relation $D_F > D_1 > \nu$ (since $dd_q/dq < 0$).

What information can be extracted by analyzing the dimensionality of a system?

1. The number of degrees of freedom n_j is given by the integral part of the fractal dimension

$$n_j = [D_F] + 1. \quad (30)$$

2. The Renyi dimensionalities are related to the singularities in the measure of the multifractal $f(\alpha)$ by (24), and also to the slope parameters (see below).

3. Fractal dimensions are related to the type of nonlinearity in the fundamental equations and effective Lagrangians. This relation is complicated, however, and can only be established numerically at present.

4. Dimensionality can provide information on the regions of enhanced dissipation, intermittency, and fractal space-time structure of the interaction region (in a quark-gluon plasma, for example).

5. Properties of cascade models are closely related to the Renyi dimension of the appropriate cascade (see Sec. 6 of this review).

6. The Renyi dimension can be employed to classify inelastic events, as long as these are treated as purely geometrical objects.

Consider this last statement.^{24,25} Each particle produced by an inelastic interaction can be represented as a point in a three-dimensional phase space which fixes the endpoint of its momentum vector. Since the transverse mo-

mentum is bounded, these points are concentrated in the so-called cylindrical phase volume centered about the longitudinal momentum components. Yet even inside this phase cylinder the point distribution is nonuniform. The geometrical characteristics of the set of points should be governed by interaction dynamics. We can attempt to classify these sets of points using Renyi dimensionality in the same manner as this is done for the Cantor set or for strange attractors. For simplicity, consider the projection of the phase volume onto the rapidity axis y and define the corresponding probabilities $p_i(l)$ in a single event as

$$p_i(l) = \frac{1}{n-1} \sum_{j \neq i} \theta(l - |y_i - y_j|), \quad (31)$$

where n is the number of particles in the event; y_{ij} are the rapidities of the i th (j th) particle normalized by the total rapidity Y . We can write the moments in the form

$$C_q(l) = \frac{1}{n} \sum_{i=1}^n p_i^q(l) = \frac{1}{n} \sum_{i=1}^n \left(\frac{1}{n-1} \sum_{j \neq i} \theta(l - |y_i - y_j|) \right)^q \quad (32)$$

and calculate the Renyi dimension from the behavior of the moments

$$C_q(l) \sim l^{qd_{q+1}}. \quad (33)$$

According to this prescription individual events can be classified using the Renyi dimension (this analysis was applied to experimental data in Ref. 27).

The finiteness of the number of particles⁶⁾ means that the limiting ($l \rightarrow 0$) form of the definition of Renyi dimensionality cannot be used, since the dimensionality of a finite number of points is always zero. As always, one should instead select a physically meaningful bin size l for the calculation of dimensionality. Different selection criteria have been proposed: Kittel and Peschanski¹⁸ suggested the same bin size $0.1 < \delta y < 1$ employed in the intermittency analysis, while Sarcevic and Satz²⁶ considered only fairly large bins $\delta y \approx 1-2$ (eliminating two-particle correlations). These procedures can lead to markedly different results, as we will

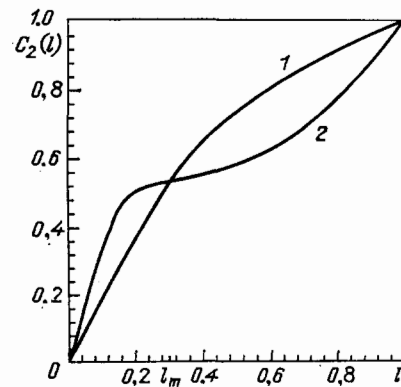


FIG. 9. Particle distribution moments of two events that produced 20 charged particles behave differently in the relatively homogeneous (monotonic curve) and strongly inhomogeneous (nonmonotonic curve) events.²⁵ This indicates that spike-containing inhomogeneous events are characterized by different fractal dimensions in large and small rapidity bins.

demonstrate using two concrete $p\bar{p}$ -interaction events^{25,27} at 400 GeV, each producing 20 charged particles. These events are chosen because in one the produced particles are quite homogeneously distributed on the rapidity axis, whereas the other produced a sharp spike of several particles in a narrow bin. The moments $C_2(l)$ for these two events are quite different (Fig. 9). In the homogeneous event $C_2(l)$ changes smoothly with l and can be approximated by a simple power-law expression with the power slightly smaller than unity. In the inhomogeneous case $C_2(l)$ contains two regions (neglecting values near unity where purely kinematic effects dominate) that can be approximated by power laws with markedly different powers. This means that inhomogeneous events with significant fluctuations cannot be treated as multifractals. Given the small multiplicities and finite statistics, it appears unhelpful to describe the regions inside and outside the spikes as different multifractals. Nonetheless, the above examples indicate that a formal fractal analysis should yield larger Renyi dimensions (i.e. smaller slope parameters) for smaller bin sizes. Moreover, the use of relatively large bins $l \sim 0.3$ makes it possible to distinguish homogeneous events from fluctuation-dominated ones and hence classify events.^{25,27} Note that if the boundary separating large and small bins is held fixed on the rapidity scale, this boundary shifts towards smaller values of reduced rapidities $l = \delta y/Y$ as energy increases. In other words, the domain of "large" bins where the single dependence is valid increases with energy.²⁶

To date it is not clear whether above-discussed properties are in any way related to the space-time structure of the interaction region, although it is tempting to assume that the distribution fractality is a consequence of the interaction region's fractal properties. This problem can be approached by various means. For example, in the study of fractal polymer chains one often investigates the diffusion of some foreign particle. The review by Sokolov²⁸ describes a mathematical model of random walks in such a polymer chain located on a plane (see Fig. 10). It is demonstrated that particle motion inside a complex object is much more convoluted than the

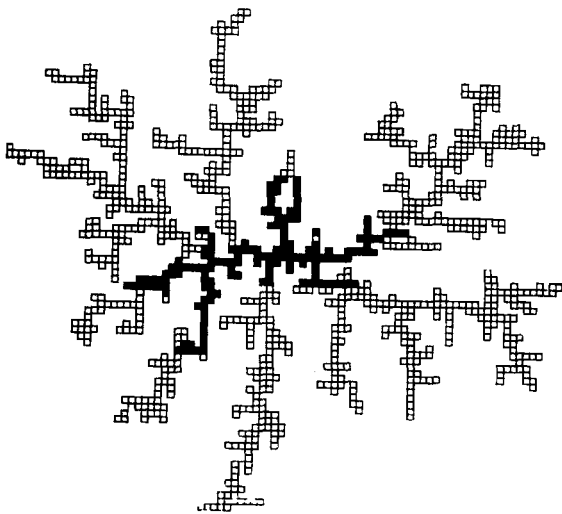


FIG. 10. Particle random walk inside a fractal (dark regions) is considerably more complicated than simple Brownian motion in a plane. The size of the dark region traversed by the particle is much smaller than expected in free Brownian motion.²⁸

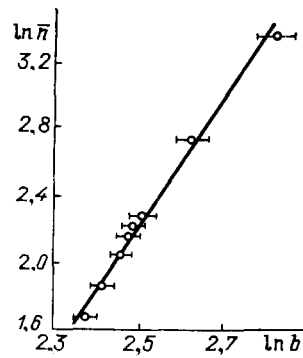


FIG. 11. Connection between diffraction cone slope and mean multiplicity leads to higher internal dimensionality of parton walks.²⁹

usual Brownian motion in a space that contains no obstacles or divisions. Even after a large number of steps the particle cannot travel far from its original position. An analog of this process in the field of inelastic interactions is the motion of the exchange parton:²⁹ in a simple multiperipheral ladder it coincides with Brownian motion in the plane normal to the collision axis. The distance of the parton in the transverse plane ρ determines the slope of the elastic diffraction cone b , while the number of steps n_0 corresponds to the multiplicity n , since each step produces a particle (resonance or cluster). In the multiperipheral ladder, as in Brownian motion, we have

$$b \sim \bar{\rho}^2 \sim t \sim n_0 \sim n, \quad (34)$$

and both b and n increase logarithmically with energy ($\sim \ln s$). Experimentally this relation between b and n is not observed, however (Fig. 11); instead it turns out²⁹ that

$$b \sim n^{2/D_w} \quad (35)$$

where for $p\bar{p}$ -interaction $D_w = 7.5 \pm 1.5$. The quantity D_w is known as the inside dimensionality of parton random walks—the fact that it is much larger than the characteristic Brownian quantity $D_w = 2$ indicates a complex trajectory of parton motion with much retracing of steps. This provides evidence of the complex fractal space-time structure of the interaction region. Here we refer the reader to the "instanton polymer vacuum" hypothesis.³⁰

Significant evidence for this picture is furnished by investigations of the shape of the deconfinement domain at the phase transition point, performed in lattice gauge theories.^{31a} It was demonstrated that the relation between the volume V and the surface area S of this region in $SU(2)$ theory is

$$V \sim S^{1.2}, \quad (36)$$

This indicates that the volume is clearly fractal and contains large "voids" filled with the "hadron" phase. The fractal dimension of the domain occupied by the "deconfinement" phase turns out to be 2.5.

Interestingly, the world lines of the monopole condensate in the confinement phase also form a fractal,^{31b} indicating their possible role in string formation. Here the fractal dimensionality of the condensate can serve as the order parameter, since it becomes unity in the "deconfinement" phase, testifying to a phase transition at the same tempera-

tures as computed previously in the studies of the number of degrees of freedom and Wilson loops.

It would appear likely that the complex structure of the interaction volume should determine the distribution of the produced particles in the phase space, just as the presence of intermittent vortices in a turbulent liquid results in a fractal structure of regions of enhanced energy emission. However, the verification of this hypothesis requires solving difficult time-dependent nonlinear problems.

6. CONNECTION BETWEEN INTERMITTENCY AND FRACTALITY

The above-discussed formulae for fractal distribution moments underscore their direct connection with intermittency properties. Moreover, it is not difficult to establish a relation between the Renyi dimension d_q and the slope parameter $\varphi(q)$.³²

$$d_q = 1 - \frac{\varphi(q)}{q-1}. \quad (37)$$

Clearly, by connecting the observed dimensionality with the geometric and thermodynamic properties of an object, the concept of fractality goes beyond a purely formal definition of intermittency. In studies of inelastic processes fractality promises to shed light on the space-time structure of the interaction region, the nature of the phase transitions, and perhaps the character of nonlinearities in the effective Lagrangian.

The spectral function $f(\alpha)$ ⁷⁾ is also widely used. It defines the multifractal distribution over fractal dimensions. For a single fractal of a given dimension $f(\alpha)$ reduces to a δ -function in the absence of fluctuations. When, in addition to self-similarity, fluctuations become important, multifractals acquire distributions of considerable width in α . As we have seen above, Renyi dimensions and slope parameters are directly related by the spectral function. This relation is summarized in the following set of formulae:

$$\begin{aligned} \varphi(q) &= f(\bar{\alpha}) + q(1 - \bar{\alpha}) - 1, \\ \frac{df}{d\alpha} \Big|_{\bar{\alpha}} &= q, \quad \frac{d^2f}{d\alpha^2} \Big|_{\bar{\alpha}} < 0, \\ \frac{d\varphi}{dq} &= 1 - \bar{\alpha}(q), \quad \frac{d^2\varphi}{dq^2} = - \left(\frac{d^2f}{d\alpha^2} \right)_{\bar{\alpha}}^{-1} > 0, \\ f(\bar{\alpha}) &= -q^2 \frac{d}{dq} \left(\frac{\varphi(q) + 1}{q} \right), \\ d_q &= \frac{1}{q-1} \left(\bar{\alpha} \frac{df}{d\alpha} \Big|_{\bar{\alpha}} - f(\bar{\alpha}) \right). \end{aligned} \quad (38)$$

Some of these formulae were derived earlier, the others can be obtained by simple transformations. They are valid in the limiting conditions where the concepts of fractality and intermittency can be defined with mathematical rigor. They can be employed in the analysis of geometric objects as well as theoretical models of particle production processes. Their practical application to inelastic processes raises the same objections we discussed earlier:

1. The transition to the limit of a vanishingly small bin size is impossible. What length scales contain information on the "real" dimensionality of the sets of points?
2. How does the finiteness of the number of points affect the results?
3. What changes if the number of points is altered?
4. How does summing over all bins in a given event

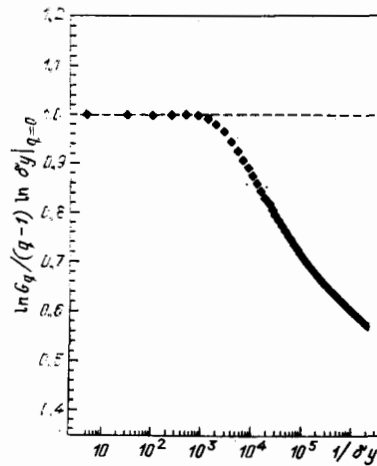


FIG. 12. Fractal dimension of a random set of 4096 points, calculated using expressions (17), (18) as a function of bin sizes l .³³

(horizontal analysis) or averaging over many events (vertical averaging) affect the results?

These questions are best answered by analyzing situations characterized by a known dimensionality.³³ For example, if a sufficiently large number of points is randomly scattered over a unit window in a uniform inclusive distribution, the actual dimensionality of a finite set of points (which is zero) will manifest itself only when the size of the covering bins l becomes noticeably smaller than the inverse number of points. At larger bin sizes the set of points will appear as a continuous line, i.e., the minimal number of bins covering the set will increase proportionally to l^{-1} as the bin size decreases—leading to an apparent "dimensionality" of one. This is explicitly demonstrated in Fig. 12, showing the results of computer calculations for a set of $2^{12} = 4096$ points.³³

The Cantor set provides an even more interesting example. The segment division process can be treated as some type of a cascade if the centers of the resulting segments are identified with "particles". By cutting off the iteration procedure after some number of iterations ν we obtain a "process" that produces 2^ν particles. We have seen already

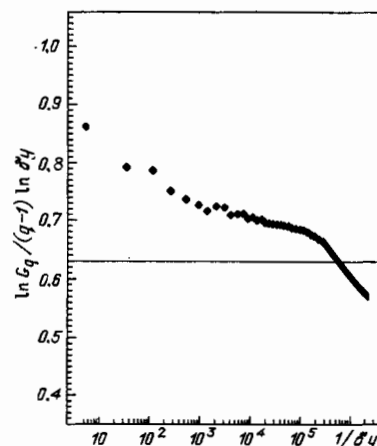


FIG. 13. True fractal dimension of the Cantor set after 12 iterations cannot be determined if the scanning of l has insufficient resolution.³³

that the fractal dimension of the Cantor set is $D_F = \ln 2 / \ln 3 \approx 0.63$. However, if the size of the covering bins is scanned in large steps, even a large number of iterations ($\nu = 12, 2^{12} = 4096$ "particles") does not suffice to give the correct dimensionality (Fig. 13). On the other hand, if the scanning is performed with fine resolution, i.e. the bin size is varied almost continuously, one obtains the "fine structure" of the above dependence and individual points yield accurate information on the fractal dimension of the set (Fig. 14).

Clearly these points correspond to cases of bin sizes being multiples of the segment lengths in the Cantor set after the given number of iterations. Consequently the distances between these points are multiples of $-\ln(1/r) = \ln 3$, where $r = 3$ is the number of segments into which an original segment is divided at each step. All moments show this structure.

Yet inelastic processes usually produce fewer particles than the example considered above. Accordingly, it is of interest to examine the Cantor set after a smaller number of iterations. Cutting off the iteration procedure after 5 iterations ($\nu = 5$) we obtain 32 "particles". We can repeat the procedure of covering this set with bins of size l , once again defining the "dimensionality" as $D_F = -d \ln N / d \ln l$, where N is the number of covering bins. By changing the size l in small steps we again obtain the same downward spikes as in the case of many iterations, where single points gave the correct dimensionality. But there is also additional "band" structure at small bin sizes with parallel and equidistant bands. This effect probably arises in inelastic processes (see below).

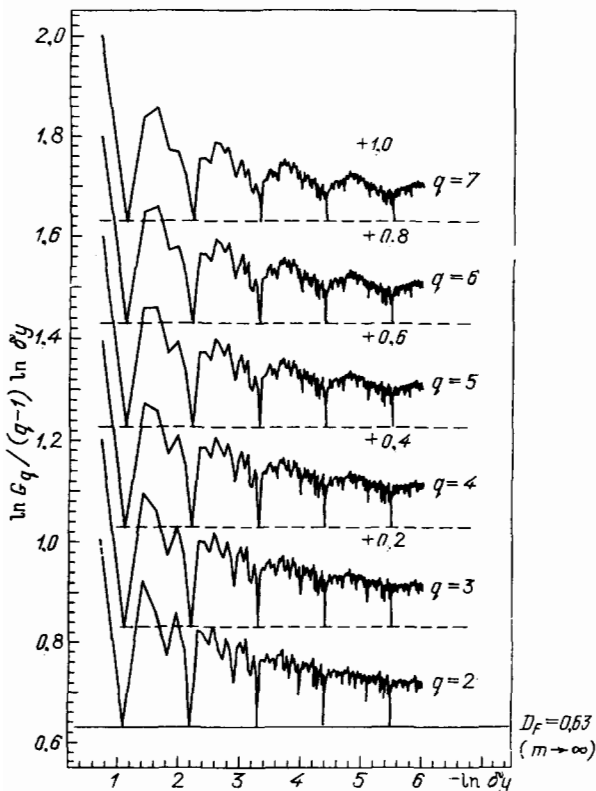


FIG. 14. If l is varied smoothly the true dimension of the Cantor set manifests itself at certain points.³³ (For clarity, different moments are shifted vertically by the amount shown in the figure).

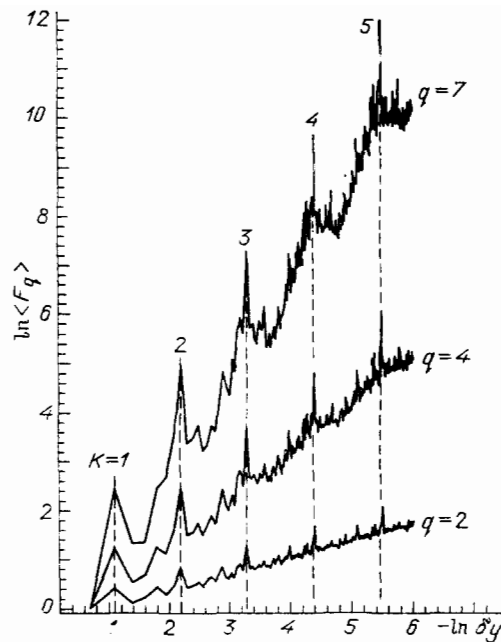


FIG. 15. Behavior of factorial moments of the Cantor set (after 12 iterations) resembles that of the fractal dimension.³³

The factorial moments of the Cantor set behave analogously. If the number of "particles" is large and the scanning of bin size proceeds in large steps, the factorial moments increase approximately linearly, whereas fine resolution in bin size reveals peaks in the factorial moments (Fig. 15). Straight lines drawn through the peak positions have slopes that are related to the fractal dimension by formula (37). Consequently factorial moments provide a means of determining the fractal dimensionality. We should note here that the slopes of straight line fits through the main groups of points in Fig. 15 are similar to lines drawn through the peaks. This argues in favor of employing factorial moments even if the bin size resolution is coarse. Evolution of the second moment as a function of iteration ("particle") number is illustrated in Fig. 16. If the particle number is large, both the peaks and the main group of points appear to lie on parallel straight lines whose slopes agree with the fractal dimension obtained from (37). If the number of particles is smaller the factorial moments fall off as the bin size decreases. In even smaller sets of particles the decaying section of the factorial moment comes to exhibit the characteristic structure of bands with slopes different from the intermittency slope parameters. At this stage it appears that the finiteness of the number of points comes into play, "activating" the zero dimension $D_F = 0$, i.e. the slopes $\varphi(q) \approx q - 1$. It remains unclear what determines the distances between the bands. Also, if the number of particles is small, the peaks tend to exaggerate the values of the intermittency slope parameters.

The same procedure can be applied to a specific inelastic π^+ p-interaction event at 250 GeV that produced 26 particles. This is the same event discussed earlier and illustrated in Fig. 4. If we ignore uncertainties in the measured positions of the particles, this event can be analyzed down to very small bin sizes $< 10^{-2}$. The second through fifth factorial moments obtained in this analysis are shown in Fig. 17.³³

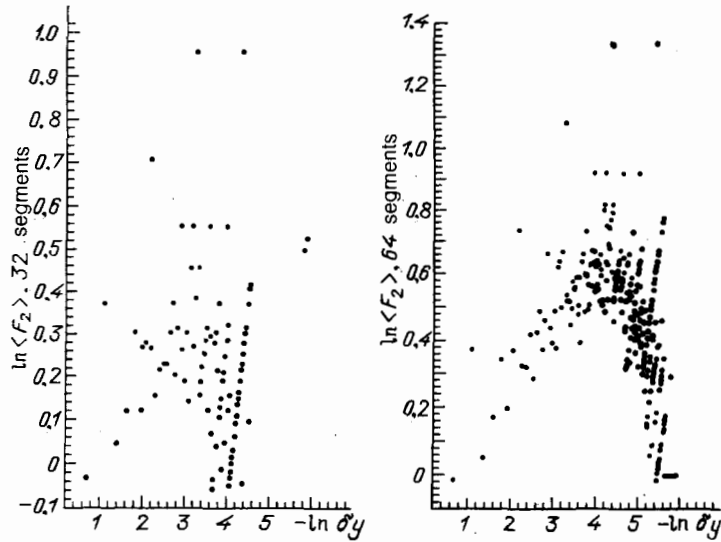
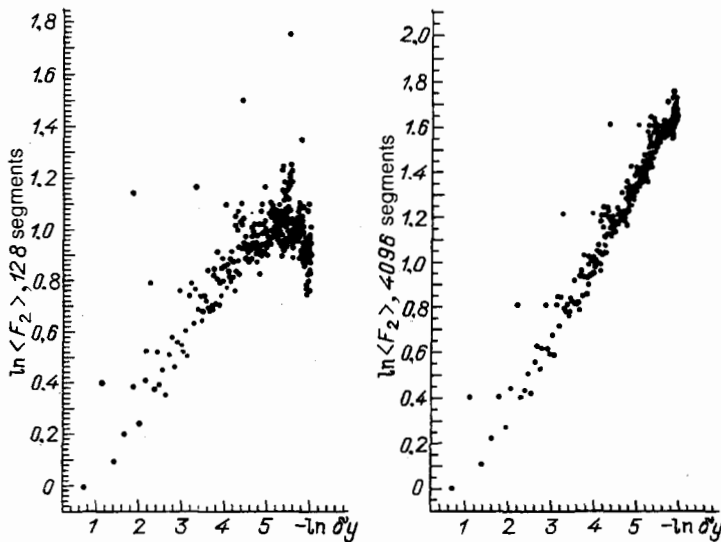


FIG. 16. Second factorial moment for different numbers of interactions of the Cantor set.



Here we find no clear peaks, although there is a group of three points on the left that might conceivably be described as such. Interestingly, the fractal dimension one obtains from these points is very close to zero, as expected from our discussion for an event with sharp spikes. At small bin sizes the band structure is evident in all moments, although the bands are no longer equidistant. Evidently the contribution of this event to lower-lying moments is so small as to be invisible on the scale of Fig. 6. But in the fifth moment, especially at small bin sizes, this event makes a dominant contribution. Clearly, by limiting the analysis to $\delta y = 0.1$, as was done in Fig. 6, one can hardly predict the band structure seen in Fig. 17 at smaller bin sizes. Only with the knowledge of band structure obtained from Fig. 17 can one attempt to discern it in the fifth moment of Fig. 6 by drawing the dotted lines.

Thus we find that even the first attempts to analyze the connection between intermittency and the fractal structure of events in phase space appear quite promising, although a complete understanding of all details is not yet available.

7. THEORETICAL MODELS

The existence of large fluctuations and, more generally, the properties of multiplicity distributions in small (pseudo) rapidity bins have always attracted scientific interest. Methods that employ factorial moments and fractal dimensions make it possible to describe these properties in a very clear fashion. Nonetheless, the efforts to connect them with many-particle correlations^{11,12} and symmetry properties of identical particles¹⁹ have not fully succeeded to date.

Generally speaking, a dynamical description of the observed phenomena in high-energy physics is still lacking, despite the multitude of hypothesis and clear analogies to other branches of physics. Since the theoretical models are obviously incomplete and limited, we will discuss them only briefly with the aim of referring the interested reader to more detailed sources in the literature.

All theoretical approaches to this problem can be tentatively classified into two groups depending on preference for ordinary or stochastic dynamics, although no clear demar-

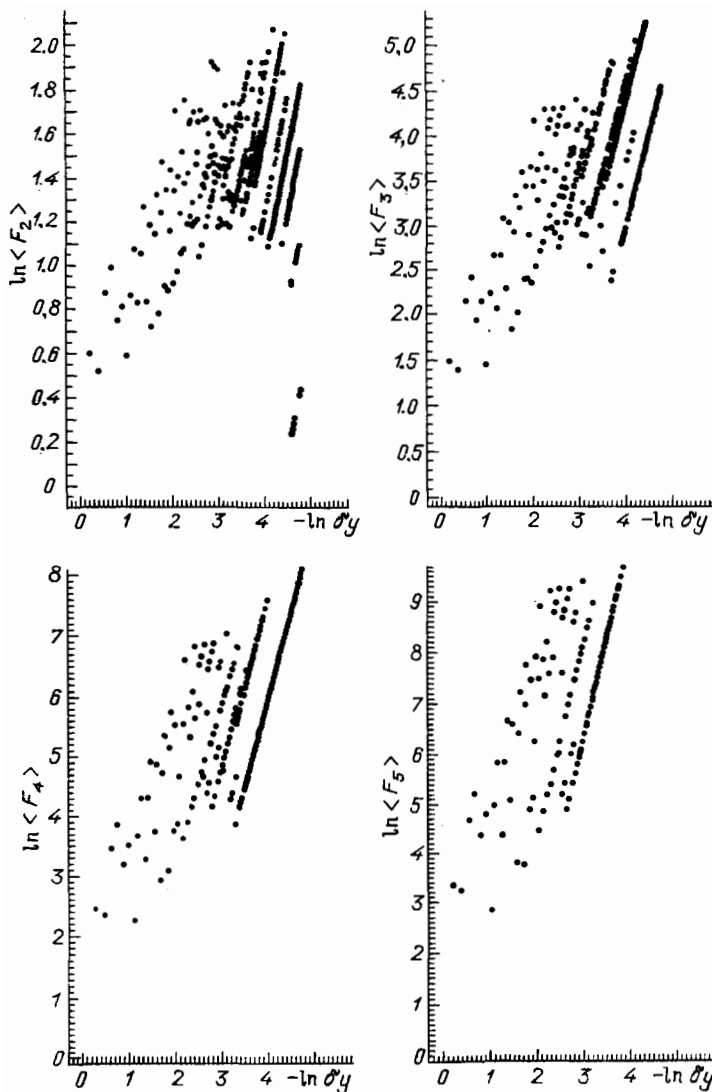


FIG. 17. Factorial moments of the single event shown in Fig. 4 calculated down to very small bin sizes.³³

cation between the two exists. The former group is comprised generally of QCD parton shower models and their phenomenological partners: the dual topological model and quark-gluon string models;^{1,3,34} cluster models;^{2,4,35,36} clan models;^{37,38} narrow hadron jet emission;³⁹ coherent gluon jet emission (Cherenkov gluons in particular);^{40,41} statistical correlations in partially coherent radiative systems;^{42,43} formation and decay of cold quark-gluon plasma.^{44,45}

The second group of models^{15,46-52} is based on analogies with turbulence theories.^{15,53} These models invoke random cascades characterized by independent probabilities and leading to phenomena resembling phase transitions.

Despite the difference in theoretical underpinnings, the imprecision of this division into two groups is obvious already from the fact that all branching processes (including QCD parton showers) lead to some degree of stochastization. In fact, the division should be attempted using some definite numerical parameter (say, the extent of stochastization).

In the plane normal to the collision axis, single events exhibiting strong particle number fluctuations in a narrow pseudorapidity bin (such as illustrated in Fig. 4) appear as

rings with relatively uniform azimuthal distributions of particles emitted at similar polar angles. Precisely for this reason the first attempts to explain the number fluctuations proceeded by analogy with Cherenkov photon radiation. The hypothesis of coherent emission of gluon jets^{40,41} (possibly involving the Vavilov-Cherenkov mechanism) predicted that these jets should be emitted in a narrow pseudorapidity bin at large angles in the center-of-mass system of the colliding hadrons. All subsequent models did not predict any particular angular dependence for the dense groups of produced particles. This specific feature was experimentally verified in $p\bar{p}$ -interactions at 205 and 360 GeV energies.⁵⁴ It turned out that the distribution of dense particle group centers on the pseudorapidity axis contained several peaks superimposed on a fairly strong background (Fig. 18). Consequently the proposed mechanism of coherent jet emission in hadron interactions probably does exist but is not dominant. The existence of another mechanism responsible for the fluctuations is indicated by their presence in electron-positron annihilation, where the necessary conditions for coherence are difficult to imagine.

Traditional models, which posited emission from ex-

change partons¹ or the breaking of quark-gluon strings,³ proved incapable initially^{13,14} of describing either the number of fluctuations and their behavior as a function of peak height, or the growth of factorial moments in small bins. Agreement with experiment probably requires initial fluctuations to accompany the breaking of each string, which would necessitate new parameters. In this regard, models based on clusters^{4,35,36} or clans^{37,38} appear more flexible, as they allow for the variation of several parameters. Van Hove demonstrated³⁸ that the existence of clans leads to a power-law increase of factorial moments in small bin sizes. No quantitative comparison with experiment was attempted, however. As for cluster models, in some cases they succeeded in describing multiplicity distributions in symmetrical rapidity bins of various sizes.^{37,38} This could prove insufficient for explaining the behavior of all factorial moments, however, since these are sensitive to the fine details that are not discernible by the usual methods of presenting distributions.

The cold quark-gluon plasma model^{44,45} has problems explaining the large values of slope parameters in electron-positron annihilation compared to hadronic and nuclear processes, since this model predicts the largest slope parameters in nuclear-nuclear collisions.

Multiparticle production is described somewhat differently in Refs. 42, 43, where new particle emission is explained by two types of sources—chaotic and coherent. Dynamical models of such sources could be constructed involving emission by virtual and leading partons respectively.

All the above approaches attempt to describe multiplicity distributions in terms of the negative binomial distribution (or some modification thereof). In the cluster model this is accomplished by varying the cluster parameters. In the clan model the negative binomial distribution is approached by convolving the Poisson distribution over the number of clans with a logarithmic distribution of decaying particles. In the statistical model with two types of sources,

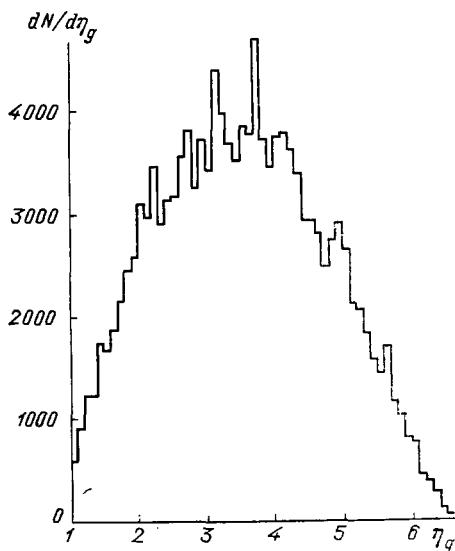


FIG. 18. Distribution of the centers of dense isolated particle groups on the pseudorapidity axis in $p\bar{p}$ -interactions at 360 GeV indicates presence of peaks on the pseudorapidity scale of ± 0.3 .⁵⁴

the negative binomial distribution naturally describes the chaotic sources, while the coherent sources contribute a Poisson component. It would appear that all these models should accurately describe the higher factorial moments by successfully fitting the lowest one. And there is a sufficient number of fitting parameters: the mean number of clans and the particles they contain; degree of chaos and the correlation length; etc.

Of course, one would expect that QCD parton showers complemented by the hadronization hypothesis will eventually describe the comprehensive experimental picture, including the intermittency phenomenon. This expectation is based on the fact that all branching processes possess fractal properties. Yet no concrete advances in this direction have been accomplished to date. Instead we are offered either purely phenomenological models of sequential branching³⁹ or investigations of the simplest theoretical models like the tree diagrams of the φ^3 model, simplified QCD^{51,52} also based on tree diagrams, or the Schwinger tunneling transition.⁵⁵ Some of the predictions are experimentally verifiable. For example, the model of sequential branching of the initial system into two rapidly moving subsystems of relatively small mass³⁹ predicts very narrow "pencil" jets consisting of groups of particles emitted into narrow polar and azimuthal angle windows. This should increase the slope parameters in a two-dimensional analysis. But experimentally^{54,70} the dense particle groups on the rapidity axis have a fairly isotropic azimuthal distribution.⁸⁾ At the same time, the slope parameters have been noted to increase when the azimuthal angle windows are further restricted.^{18,69,70} This requires a detailed study of particle group definitions, etc.

An analysis of the equations of the branching processes^{51,52} in the uniform division model, in the φ^3 theory, and in the first logarithmic QCD approximation, indicates that the totality of produced partons exhibits intermittency and can be subjected to the full multifractal analysis described earlier. The slope parameters depend on the concrete form of the kernel of the integral equation which describes the process. They prove to be quite significant in e^+e^- -annihilation^{29,56} if the hadronization of partons is assumed to have little effect. In this case the singularity spectrum of $f(\alpha)$ [see (22)] is wider than in the φ^3 model because of the broader rapidity distribution.⁵² By incorporating an integral of multiplicative terms the iterative solution of the branching equations should lead to stochastization. The complexity of the solution, however, has hindered the derivation of clear stochastization criteria. For this reason the simplified cascade models constructed by analogy with turbulence¹⁵ have proved to be more popular.

The random cascade models involve some probability distribution $r(W)$ with corresponding moments:

$$\langle W^q \rangle = \int dW r(W) W^q, \quad \langle 1 \rangle = \langle W \rangle = 1. \quad (39)$$

These probabilities govern the fluctuations as the rapidity window is broken up into ever smaller bins. The probability P_m of appearing in the m th bin is given by the multiplicative expression

$$P_m = \frac{1}{M} \sum_{n=1}^{\nu} W_n, \quad (40)$$

where $M = \lambda^\nu$ is the number of bins obtained by breaking up each bin into λ parts at each of the ν iterations. In this pro-

cess a sequence of indices n leads precisely to a predetermined bin m . The multiplicative form of expression (40) naturally results in large fluctuations and intermittency.

The simplest type of distribution $r(W)$ is the so-called α -model given by

$$r(W) = p\delta(W-a) + (1-p)\delta(W-b), \quad (41)$$

where $0 \leq a < 1 < b$ and $pa + (1-p)b = 1$ because of the normalization condition (39). This model was widely used in turbulence theory, as well as in the theory of spin glasses. As the parameters p and λ are changed the model predicts various phase transitions. Interestingly, intermittency of domains with ordered spins also appears in the two-dimensional Ising model near the phase transition.^{57,58} We should again recall the fractal structure of the deconfinement phase,³¹ discussed earlier in this review.

On the whole, cascade models are presently at the point of evaluating the qualitative results and cannot be compared with experiment because of difficulties in treating the finite number of particles, conservation laws, etc. The proposed versions which take these requirements into account⁵⁹ currently fix their parameters by turning to experimental data. They point to the necessity of complementing string models with initial fluctuations in the breaking of each string.

In the limiting case of a large number of cascades the product of independent probabilities in expression (40) should produce a log-normal distribution.^{60,74,75} Factorial moments furnish information on the tail of this distribution. Distribution parameters and properties in the main body of this distribution will require logarithmic moments of the $\langle \ln n \rangle_q$ variety.⁶⁰ It is not clear what energies will be required to reach this limiting case.⁹⁾

8. CONCLUSION

I would like to conclude this review by noting that the details of the theoretical computations have been omitted for the sake of brevity. I attempted to present the fundamental ideas and discuss their interconnections in a concise form. The brevity of this review—really a list of theoretical models—is also motivated by the fact that these models are far from complete. Currently they are designed to establish quantities like fractality and intermittency slope parameters only. The modest goals of these models are evident in the proposals for bringing more advanced Monte Carlo models of showers into conformity with experiment by establishing a new stochastic dynamics or determining the effective Lagrangians that govern particle production at high energies. The hydrodynamic theory of multiparticle production is yet to speak on this subject.

The future will tell which of these approaches will prove the most productive. For now it is clear only that the concepts of slope parameters and fractality have ignited new interest in the problem of correlations in multiparticle production processes and brought forth new ideas on the dynamics of these processes.

given event (horizontal) and over an ensemble of events in a given bin (vertical) are discussed in detail by Hwa.¹⁶ Mathematicians refer to factorial moments as the empirical assessment of ordinary moments.

⁴⁾ For convenience of the reader the references cite experimental studies⁶¹⁻⁷³ that complement the earlier work⁵⁻⁹ discussed in the review.

⁵⁾ The difference between the two definitions is not relevant to our topic and we will omit a detailed discussion.

⁶⁾ The significance of this effect will be discussed in the following section.

⁷⁾ For example, to reveal phase transitions in the linear ranges of this function.

⁸⁾ The contribution of jets with large transverse momenta is small and their width is usually quite large, much larger than 0.1.

⁹⁾ Ingelman⁷⁴ has suggested that the logarithmically normal distribution suffices to describe multiplicity distributions in the total rapidity window at high energies. In smaller rapidity bins, however, one runs into a problem with empty bins ($n = 0$).⁷⁵

¹⁾ a) A. Capella and J. Tran Thanh Van, *Z. Phys. C* **38**, 177 (1988); b) A. Capella, in *Proc. 18th Intern. Symp. on Multiparticle Dynamics*, Tashkent, USSR, 1987, p. 129.

²⁾ C. Fuglesang, in *Proc. 19th Intern. Symp. on Multiparticle Dynamics*, Arles, France, 1988, p. 257.

³⁾ B. Andersson *et al.*, *Nucl. Phys. B* **281**, 289 (1987).

⁴⁾ I. M. Dremin and A. M. Dunaevskii, *Phys. Rep.* **18**, 159 (1975); I. M. Dremin, in: *Proc. 12th Intern. Symp. on Multiparticle Dynamics*, Notre Dame, U. S., 1981, p. 261.

⁵⁾ K. I. Alekseeva *et al.*, *Zh. Eksp. Teor. Fiz.* **43**, 783 (1962) [*Sov. Phys. JETP* **16**, 554 (1963)]; *Izv. Akad. Nauk SSSR, Ser. Fiz.* **26**, 572 (1962) [*Bull. Acad. Sci. USSR*, **26**, No. 5, 571 (1962)].

⁶⁾ N. Arata, *Nuovo Cimento A* **43**, 455 (1978).

⁷⁾ A. V. Apanasenko *et al.*, *Pis'ma Zh. Eksp. Teor. Fiz.* **30**, 157 (1979) [*JETP Lett.* **30**, 145 (1979)].

⁸⁾ N. A. Marutyan *et al.*, *Yad. Fiz.* **29**, 1566 (1979) [*Sov. J. Nucl. Phys.* **29**, 804 (1979)].

⁹⁾ M. Adamus *et al.*, *Phys. Lett. B* **185**, 200 (1987).

¹⁰⁾ I. M. Dremin, preprint CERN-TH 4693/87, Geneva, 1987.

¹¹⁾ P. Carruthers and I. Sarcevic, *Phys. Rev. Lett.* **63**, 1562 (1989).

¹²⁾ A. Capella *et al.*, *Phys. Lett. B* **230**, 149 (1989).

¹³⁾ R. Peschanski and J. Tran Thanh Van, in *Proc. 18th Intern. Symp. Multiparticle Dynamics*, Tashkent, USSR, 1987.

¹⁴⁾ B. Andersson *et al.*, in *Proc. 19th Intern. Symp. on Multiparticle Dynamics*, Arles, France, 1987.

¹⁵⁾ A. Bialas and R. Peschanski, *Nucl. Phys. B* **273**, 703 (1986).

¹⁶⁾ R. C. Hwa, preprints OITS 407, 412, 1989.

¹⁷⁾ L. Van Hove, *Mod. Phys. Lett. A* **4**, 1867 (1989); preprint CERN-TH 5529/89, Geneva, 1989.

¹⁸⁾ W. Kittel and R. Peschanski, in *Proc. EPS Conf.*, Madrid, 1989.

¹⁹⁾ M. Gyulassy, preprint LBL-26831, 1989.

²⁰⁾ I. V. Andreev, in *Proc. CAMP Intern. Conf.*, Marburg, Germany, 1990, World Scientific, Singapore, 1990, p. 156.

²¹⁾ I. V. Andreev, *Pis'ma Zh. Eksp. Teor. Fiz.* **33**, 384 (1981) [*JETP Lett.* **33**, 367 (1981)].

²²⁾ G. Paladin and A. Vulpiani, *Phys. Rep.* **156**, 147 (1987).

²³⁾ A. Renyi, *Probability Theory*, North-Holland, Amsterdam, 1970.

²⁴⁾ I. M. Dremin, *Mod. Phys. Lett. A* **3**, 1333 (1988).

²⁵⁾ I. M. Dremin, *Mod. Phys. Lett. A* **4**, 1027 (1989).

²⁶⁾ I. Sarcevic and H. Satz, preprints AZPH-TH/89-58, BNL-43183, 1989.

²⁷⁾ I. M. Dremin, preprint FNAL-89/71-T, 1989; in *Leon Van Hove Festschrift*, World Scientific, Singapore, 1990, p. 418.

²⁸⁾ I. M. Sokolov, *Usp. Fiz. Nauk* **150**, 221 (1986) [*Sov. Phys. Usp.* **29**, 924 (1986)].

²⁹⁾ I. M. Dremin, *Pis'ma Zh. Eksp. Teor. Fiz.* **45**, 505 (1987) [*JETP Lett.* **45**, 643 (1987)].

³⁰⁾ E. V. Shuryak, *Phys. Rep.* **115**, 153 (1984).

³¹⁾ a) M. I. Polikarpov, *Phys. Lett. B* **236**, 61 (1990); b) U. E. Wiese and M. I. Polikarpov, preprint IFUP-TH, 1989.

³²⁾ P. Lipa and B. Buschbeck, *Phys. Lett. B* **223**, 465 (1988).

³³⁾ B. Levchenko, preprint MPI, 1990.

³⁴⁾ A. B. Kaidalov, *Phys. Lett. B* **116**, 459 (1982).

³⁵⁾ L. S. Liu and T. C. Meng, *Phys. Rev. D* **27**, 2640 (1983).

³⁶⁾ Cai Xu *et al.*, *Phys. Rev. D* **33**, 1287 (1986).

³⁷⁾ A. Giovannini and L. Van Hove, *Acta Phys. Pol. B* **19**, 495, 917, 931 (1988).

³⁸⁾ L. Van Hove, preprint CERN-TH 5563/89, Geneva, 1989.

³⁹⁾ W. Ochs and J. Wosiek, *Phys. Lett. B* **214**, 617 (1988).

⁴⁰⁾ I. M. Dremin, *Pis'ma Zh. Eksp. Teor. Fiz.* **30**, 152 (1980) [*JETP Lett.* **30**, 140 (1980)].

⁴¹⁾ I. M. Dremin, *Fiz. Elem. Chastits At. Yadra* **18**, 79 (1987) [*Sov. J. Part. Nucl.* **18**, 31 (1987)].

⁴²⁾ G. N. Fowler and R. M. Weiner, *Phys. Rev. D* **17**, 3117 (1978).

⁴³⁾ P. Carruthers *et al.*, preprint AZPH-TH/89-1, 1989.

¹⁾ Here we refer to a version of the model that allows several "ladders".

²⁾ The square brackets around $de(y)$ indicate a functional.

³⁾ We should note that formula (12) employed by experimentalists differs somewhat from the result of the Bialas and Peschanski.¹⁵ The latter reduces to (12) in events with multiplicity significantly exceeding the order q , more precisely when $n \gg q - 1$. The order of averaging over a

- ⁴⁴L. Van Hove, *Ann. Phys. (N.Y.)* **192**, 66 (1989).
⁴⁵D. Seibert, *Phys. Rev. Lett.* **63**, 136 (1989).
⁴⁶A. Bialas and R. Peschanski, *Nucl. Phys. B* **308**, 357 (1988); *Phys. Lett. B* **207**, 59 (1988).
⁴⁷P. Peschanski, *Nucl. Phys. B* **327**, 144 (1989).
⁴⁸A. Desvallees *et al.*, preprint SPhT/89-138, 1989.
⁴⁹Ph. Brax and R. Peschanski, preprint SPhT/89-203, 1989.
⁵⁰A. Bialas *et al.*, preprint TPJU-16/89, 1989.
⁵¹R. C. Hwa, preprint OITS-404, 1989.
⁵²C. B. Chiu and R. C. Hwa, preprints OITS-424, 1989; OITS-431, 1990.
⁵³J. Dias de Deus, *Phys. Lett. B* **194**, 297 (1987).
⁵⁴I. M. Dremin *et al.*, *Yad. Fiz.* **51** (1990) [*Sov. J. Nucl. Phys.* **51** (1990)].
⁵⁵A. Bialas *et al.*, preprints TPJU-13/89, 1989; SPhT/89-96, 1989.
⁵⁶K. Fialkowski *et al.*, preprint TPJU-6/89, 1989.
⁵⁷H. Satz, preprint CERN-TH 5312/89, Geneva, 1989.
⁵⁸R. Peschanski, preprint SPhT/89-132, 1989.
⁵⁹A. V. Leonidov and M. M. Tsy-pin, *Mod. Phys. Lett. A* **8**, 1256 (1990).
⁶⁰I. M. Dremin, *Mod. Phys. Lett. A* **4**, 2685 (1989).
⁶¹T. H. Burnett *et al.*, *Phys. Rev. Lett.* **50**, 2062 (1983).
⁶²G. J. Alner *et al.*, *Phys. Rep.* **154**, 247 (1987).
⁶³M. Adamus *et al.*, *Phys. Lett. B* **188**, 113 (1987).
⁶⁴M. I. Adamovich *et al.*, *Phys. Lett. B* **201**, 397 (1988).
⁶⁵E. Stenlund *et al.*, preprint LUIP 8807, 1988.
⁶⁶A. Bamberger *et al.*, *Phys. Lett. B* **203**, 320 (1988); **205**, 583 (1988).
⁶⁷A. Bamberger *et al.*, *Z. Phys. C* **43**, 25 (1989).
⁶⁸R. Holynski *et al.*, *Phys. Rev. Lett.* **62**, 733 (1989).
⁶⁹W. Braunschweig *et al.*, preprint DESY 89-092, Hamburg, 1989.
⁷⁰N. Ajinenko *et al.*, *Phys. Lett. B* **222**, 306 (1989).
⁷¹I. Derado, in *Leon Van Hove Festschrift*, World Scientific, Singapore, 1990.
⁷²B. Buschbeck, in *Leon Van Hove Festschrift*, World Scientific, Singapore, 1990.
⁷³E. Gladysz-Dziadus, preprint Krakow, 1989.
⁷⁴G. Ingelman, in *Proc. XXIV Moriond Conf.*, March 11-17, 1990 (J. Tran Thanh Van, editor), Editions Frontieres, Paris, 1990, p. 182.
⁷⁵I. M. Dremin *et al.*, preprint Wuhan HZPP-89-15, 1989.

Translated by A. Zaslavsky